ChemComm

COMMUNICATION

View Article Online
View Journal | View Issue

Check for updates

Cite this: *Chem. Commun.*, 2021, 57, 8925

Received 20th July 2021,
Accepted 9th August 2021

DOI: 10.1039/d1cc03919a

rsc.li/chemcomm

Open Access Article. Published on 09 August 2021. Downloaded on 1/17/2026 9:00:54 AM.
This article is licensed under a Creative Commons Attribution 3.0 Unported Licence.

[Fe_{15}]: a frustrated, centred tetrakis hexahedron†

Daniel J. Cutler, [a] Mukesh K. Singh, [a] Gary S. Nichol, [a] Marco Evangelisti, [b] Jürgen Schnack, *[c] Leroy Cronin *[d] and Euan K. Brechin *[a]

The combination of two different Fe^{III} salts in a solvothermal reaction with triethanolamine results in the formation of a high symmetry [Fe^{III}_{15}] cluster whose structure conforms to a centred, tetrakis hexahedron.

Homometallic compounds of Fe^{III} have played a central role in the history of molecular magnetism, proving key to the development and understanding of an array of physical properties. For example, the study of oxo-bridged [Fe_2] dimers allowed the development of detailed magneto-structural correlations that can be translated to larger species,[1] antiferromagnetically coupled [Fe_{6-12}] ferric wheels revealed interesting quantum size effects manifested in stepped magnetisation,[2] [$Fe_{17/19}$] was an early example of a molecule possessing a very large spin ground state,[3] [Fe_8] was the second known example of a single-molecule magnet,[4] [Fe_{14}] was an early example of a compound displaying an enhanced magnetocaloric effect,[5] and cages ranging in nuclearity from [Fe_{13}] to [Fe_{34}] have structures that conform to Archimedean and Platonic solids which aid understanding of the self-assembly of molecular oxides en route to mineral phases.[6] High symmetry clusters are of particular interest as they may possess geometric spin frustration, a phenomenon whose definition has evolved from its strict initial derivation.[7] Frustration can lead to some unusual and potentially useful low-temperature physics, a beautiful example being the [$Mo_{72}Fe_{30}$] icosidodecahedron which shows anomalous magnetisation behaviour in an applied magnetic field.[8]

One synthetic methodology proven to enable the construction of such species is hydro/solvothermal synthesis, which typically exploits superheating reaction solutions under autogenous pressure.[9] In the chemistry of polynuclear cluster compounds of paramagnetic transition metal ions, the temperature regimes employed (which are typically below 250 °C) can lead to enhanced solubility, reduced solvent viscosity and increased reagent diffusion. The result is often the synthesis of metastable kinetic products of high symmetry, with slow cooling enabling pristine crystal growth directly from the reaction mixture.[10]

The solvothermal reaction of $FeCl_3$, $Fe(ClO_4)_3{\cdot}6H_2O$ and $teaH_3$ (triethanolamine) in a basic MeOH solution results in the formation of red/brown crystals upon cooling (see the Experimental section in the ESI† for full details). Crystals of [$Fe^{III}_{15}O_6(tea)_8Cl_6$](OH)($ClO_4$)$_2$ (**1**, Fig. 1 and Fig. S1, Table S1, ESI†) were found to be in a trigonal crystal system, and structure solution was performed in the $R\bar{3}$ space group (see the Crystallographic section in the ESI† for full details). The metallic skeleton of **1** describes a centred tetrakis hexahedron (Fig. 2), a Catalan solid which is the dual of the truncated octahedron, an Archimedean solid. The central Fe ion (Fe4) is octahedral, being bonded to six oxide ions ([FeO_6]; O5 and symmetry equivalent; Fe–O5 = 1.999 Å). O5 bridges to two further Fe ions in the peripheral shell (O5–Fe1 = 1.925 Å; O5–Fe2 = 2.025 Å) and is thus three coordinate and trigonal planar. There is a fourth, longer contact to Fe3 (O5–Fe3 = 2.492 Å), so O5 may be considered pseudo-tetrahedral if one considers this interaction significant (Fig. 2 and Fig. S2, S3, ESI†). The outer shell is decorated with a combination of halide and tea^{3-} ions. The former are monodentate, coordinated to Fe2 (Fe2–Cl, 2.315 Å). The latter are tetradentate, chelating either Fe1 or Fe3 with each O-atom μ-bridging to a second Fe ion (Fe2). Thus Fe1 is five-coordinate ([FeO_4N]) and trigonal pyramidal, Fe2 is six-coordinate ([FeO_5Cl]) and octahedral, and Fe3 is four coordinate ([FeO_3N]) and trigonal prismatic, or seven coordinate ([FeO_6N])

[a] *EaStCHEM School of Chemistry, The University of Edinburgh, David Brewster Road, Edinburgh, EH9 3FJ, Scotland, UK. E-mail: ebrechin@ed.ac.uk*
[b] *Instituto de Nanociencia y Materiales de Aragón (INMA), CSIC – Universidad de Zaragoza, 50009 Zaragoza, Spain*
[c] *Fakultät für Physik, Universität Bielefeld, Postfach 100131, D-33501 Bielefeld, Germany. E-mail: jschnack@uni-bielefeld.de*
[d] *School of Chemistry, The University of Glasgow, Joseph Black Building, Glasgow, G12 8QQ, Scotland, UK. E-mail: lee.cronin@glasgow.ac.uk*

† Electronic supplementary information (ESI) available: Experimental procedures, X-ray diffraction data, computational details. CCDC 2090901. For ESI and crystallographic data in CIF or other electronic format see DOI: 10.1039/d1cc03919a

Open Access Article. Published on 09 August 2021. Downloaded on 1/17/2026 9:00:54 AM.
This article is licensed under a Creative Commons Attribution 3.0 Unported Licence.

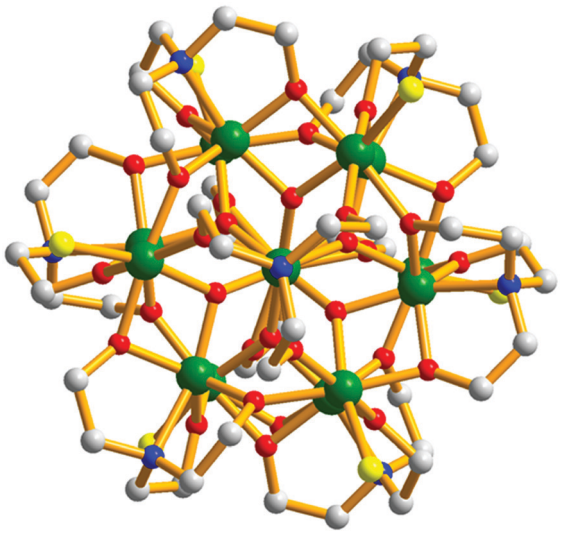

Fig. 1 Molecular structure of the cation of **1** viewed down the *c*-axis of the unit cell. Colour code: Fe = green, O = red, N = blue, C = grey, Cl = yellow. H atoms omitted for clarity.

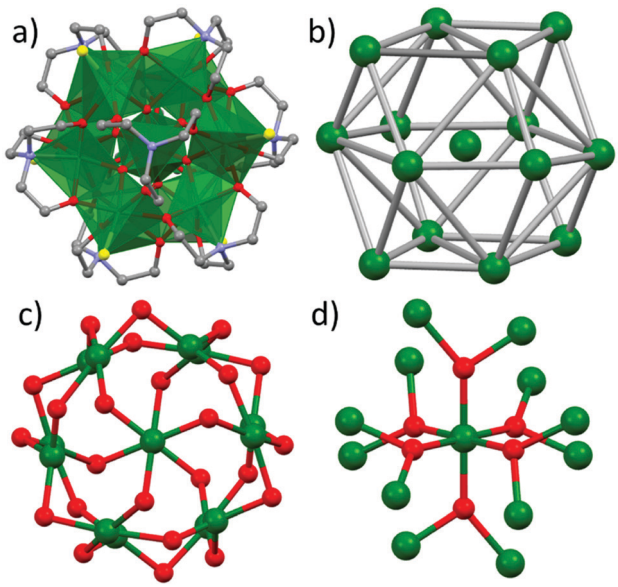

Fig. 2 Different views of the structure of the cation of **1**. (a) The molecular structure of the cation of **1** viewed down the *c*-axis of the unit cell with the metal ions drawn in polyhedral format. (b) The metallic skeleton, which conforms to a [centred] tetrakis hexahedron. The $[M_{15}O_6]^{33+}$ metal-oxide core, highlighting (c) the Fe–O connectivity in the outer shell of the molecule *via* the bridging alkoxides, and (d) the link between the central Fe ion and the outer shell *via* the six μ_3-oxide ions. Fe = green, O = red, N = blue, C = grey, Cl = yellow. H atoms omitted for clarity.

and a capped octahedron if the Fe–O5 bonds are included (Fig. S3 and S4, ESI†). A review of the Cambridge Structural Database (CSD) for Fe–O bond lengths in any Fe–O–Fe moiety produces 3378 different compounds and 12 361 bond lengths ranging from a minimum value of 1.651 Å to a maximum value of 2.629 Å, as depicted in the histogram in Fig. S5 (ESI†).

The $[Fe_{15}O_{30}]$ core displays a breadth of different Fe–O–Fe angles, ranging from a minimum of 86.67° (Fe4–O5–Fe3) to a maximum of 140.82° (Fe4–O5–Fe2). Angles from the central Fe4 ion to the peripheral Fe1 and Fe2 ions *via* the O5 oxide are 140.82° and 117.41°, while those connecting the outer Fe1, Fe2 and Fe3 ions together *via* the oxides and alkoxides range between 86.7–129.39° (Table S2, ESI†). The closest intermolecular interactions are between the monodentate Cl ions on Fe2 and the C-atoms of the tea^{3-} ligands on neighbouring molecules (Cl1···C7, ~3.43 Å), and between the perchlorate O-atoms and the C-atoms of the tea^{3-} ligands (O6···C4, ~3.43 Å; Fig. S6 and S7, ESI†). This results in an aesthetically pleasing honeycomb-like network when viewed down the *c*-axis of the cell. A search of the CSD reveals that just three $[Fe_{15}]$ clusters have been reported previously,[11] with **1** being the first example of a [centred] tetrakis hexahedron. Perhaps more surprisingly, given the widespread use of the H_3tea ligand in 3d coordination chemistry, there are very few homometallic Fe^{III} clusters of this ligand deposited. Indeed, they are limited to $[Fe_5]$,[12] $[Fe_6]$ wheels (both unsupported[13] and supported[14]), $[Fe_7]$,[15] $[Fe_8]$[16] (including an $[Fe_8]$ cluster self-assembled into a $[Fe_{64}]$ cage[17]), and $[Fe_{10}]$.[18] Heterometallic Fe–Ln species are far more prevalent.[19]

The direct-current (dc) molar magnetic susceptibility, χ, of a polycrystalline sample of **1** was measured in an applied magnetic field, B, of 0.1 T, over the 2–300 K temperature, T, range. The results are plotted in Fig. 3 in the form of χT product, where $\chi = M/B$ with M the magnetisation. At room temperature, the χT product is 28.67 emu K mol^{-1}, much lower than the Curie constant expected for fifteen uncorrelated $S = 5/2$ centres (65.625 emu K mol^{-1}) with $g = 2$. On lowering the temperature, the χT product decreases rapidly, reaching a value of 11.05 emu K mol^{-1}) at $T = 10$ K, before decreasing even more abruptly to a value of 7.74 emu K mol^{-1} at $T = 2$ K. The data is therefore indicative of competing antiferromagnetic exchange interactions, and a ground state spin of $S \approx 9/2$ (compare arrows in Fig. 3). Variable-temperature-variable-field (VTVB) dc magnetisation measurements in the temperature range 2–6 K and in applied magnetic fields up to 7 T reach a maximum value of just $M = 8.35$ μ_B (Fig. 3b), well below the upper limit expected for a ferromagnetically coupled system ($M = 75$ μ_B for $g = 2$). This behaviour is clearly indicative of relatively strong antiferromagnetic interactions between the Fe^{III} ions, consistent with the Fe–O distances and Fe–O–Fe angles present.[1]

It is computationally impossible to quantitatively analyse the magnetic data of a molecule containing $15 \times S = 5/2$ spins *via* conventional matrix diagonalisation techniques since the dimension of the Hilbert space is 470,184,984,576 and thus we turn to the finite-temperature Lanczos method.[20] Even here, several assumptions must be made. (A) Despite the presence of eight independent exchange interactions, we reduce this to four based on similar Fe–O bond lengths and Fe–O–Fe angles (Fig. S8, ESI†). These are: J_{cube} along edges of the cube; $J_{pyramid}$ along the four edges from the top of each pyramid to the respective base square of the cube; $J_{c,cube}$ from the central Fe inside the cube to vertices of the cube; and $J_{c,pyramid}$ from the

 This journal is © The Royal Society of Chemistry 2021

Open Access Article. Published on 09 August 2021. Downloaded on 1/17/2026 9:00:54 AM.
This article is licensed under a Creative Commons Attribution 3.0 Unported Licence.

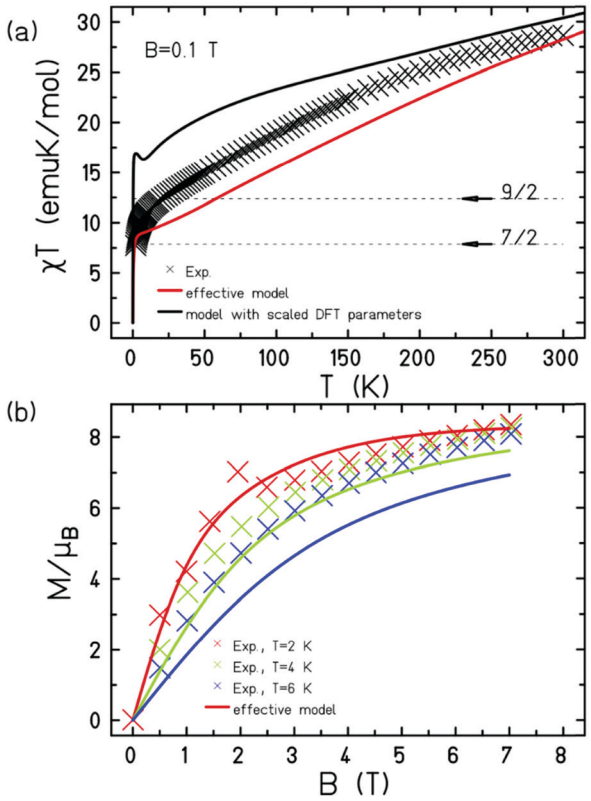

Fig. 3 (a) Magnetic susceptibility (χT) *versus* temperature (T) data for **1** measured in an applied field, B = 0.1 T in the T = 300–2 K temperature range. (b) Magnetisation (M) *versus* field (B) data in the 2–6 K temperature and 0–7 T field ranges. The solid lines are a simulation of the experimental data (x) using the finite-temperature Lanczos method. The effective model denotes a Heisenberg model with high symmetry, as described in the main text. The black line in (a) denotes the model employing DFT parameters given in Table S3 (ESI†) in a Heisenberg model scaled by 25/9 taking into account the use of spins, S = 3/2.

central Fe ion to the tops of pyramids. (B) We simulate the data using isotropic S = 3/2 spins rather than isotropic S = 5/2 spins and scale the resulting data accordingly. The corresponding isotropic spin-Hamiltonian is:

$$\hat{H} = -2\sum_{i<j} J_{ij}\hat{\vec{s}}_i \cdot \hat{\vec{s}}_j$$

where J_{ij} denotes the four employed exchange constants, respectively. A rather good theoretical representation of the data (Fig. 3) was obtained with J_{cube} = −17.4 cm^{-1}, J_{pyramid} = −17.4 cm^{-1}, $J_{\mathrm{c,cube}}$ = −17.4 cm^{-1} and $J_{\mathrm{c,pyramid}}$ = −3.5 cm^{-1}, scaled by 9/25 to meet a Hamiltonian with spins S = 5/2. Such a scaling approach can only provide "an order of magnitude" estimate of the exchange constants, rather than a precise derivation, albeit the numbers are entirely consistent with experimentally and computationally derived magneto-structural correlations for O-bridged Fe^{III} clusters.[21] The exchange constants are indicative of a highly frustrated system, as one might expect from the structural symmetry. Heat capacity, C, measurements were collected between ∼0.3 K and 30 K, for B = 0, 3 and 7 T (Fig. S9, ESI†). Below ∼3 K, the heat capacity depends significantly on B, the zero-field C showing essentially flat behaviour and reaching values close to ∼0.5R, where R is the gas constant. This behaviour is similar to that recently reported for an [$Fe^{III}_{10}Gd^{III}_{10}$] wheel[22] and consistent with the presence of a large density of low-lying states, likely resulting from competing antiferromagnetic interactions.

To further support the relative sign and magnitude of the coupling constants obtained, we have performed DFT calculations (see the ESI† for the Computational details) on a model complex, **1A**, derived from complex **1** (Fig. S10 and S11, ESI†). These suggest that the eight independent exchange interactions are in the range $|J|$ = 4.6–16.4 cm^{-1} (Table S3, ESI†), in good agreement with the experimental simulations. All are antiferromagnetic in nature, with the exception of the Fe4–(μ_4-O^{2-})$_3$–Fe3 interaction which affords J = +4.6 cm^{-1} on account of the large Fe–O bond lengths and small Fe–O–Fe bond angles present which lead to orbital orthogonality. Overlap integral calculations[23] using metal-based singly occupied molecular orbitals (SOMOs) reveal that the strongest antiferromagnetic interactions occur where there are a higher number of strong or moderate overlap integrals, and *vice versa* (Fig. S12 and S13, ESI†). For the Fe4–(μ_4-O^{2-})$_3$–Fe3 interaction (J_1 in Tables S3 and S4, ESI†) there is only one strong interaction ($d_{z^2}||d_{xz}$) with the remaining 24 interactions being weak. The overall result is a weak/moderate ferromagnetic interaction. See the ESI† for more information. Spin density analysis suggests that strong spin delocalisation is present in **1** with Fe^{III} spin densities ranging between 4.007–4.151 (Fig. S14, ESI†).

It is somewhat unusual for synthetic chemists to employ two different metal salts for the formation of homometallic cluster compounds containing paramagnetic 3d metals, since the anions are often considered solely as charge balancing moieties rather than structure-directing agents. This observation has certainly prompted us to re-examine a number of reactions to probe whether it may be of general applicability, or if it is of more limited scope. Here, the use of both $FeCl_3$, $Fe(ClO_4)_3\cdot 6H_2O$ with $teaH_3$ in a high temperature, high pressure reaction leads to the formation of an aesthetically pleasing [Fe_{15}] cage conforming to a centred, tetrakis hexahedron. The high symmetry of the metallic skeleton leads to the presence of competing antiferromagnetic exchange interactions and spin frustration. Use of the finite temperature Lanczos method allows for "an order of magnitude" estimation of the exchange constants present, a computationally non-trivial task for a molecule containing fifteen S = 5/2 spins. Values of J_{cube} = −17.4 cm^{-1}, J_{pyramid} = −17.4 cm^{-1}, $J_{\mathrm{c,cube}}$ = −17.4 cm^{-1} and $J_{\mathrm{c,pyramid}}$ = −3.5 cm^{-1} are consistent with parameters obtained from DFT calculations which fall in the range +4.6 to −16.4 cm^{-1}, and with low temperature heat capacity data which reflects the presence of a large density of low-lying spin states.

EKB and LC thank U21/EPSRC for funding a studentship (DJC). MKS would like to thank Edinburgh Compute and Data Facility (ECDF), and the European Union Horizon 2020 research and innovation programme under the Marie Skłodowska-Curie grant agreement no. 832488. ME thanks the Spanish Ministry of Science and Innovation (Project RTI2018-098537-B-C22).

Open Access Article. Published on 09 August 2021. Downloaded on 1/17/2026 9:00:54 AM.
This article is licensed under a Creative Commons Attribution 3.0 Unported Licence.

Conflicts of interest

There are no conflicts to declare.

Notes and references

1 H. Weihe and H. U. Güdel, *J. Am. Chem. Soc.*, 1998, **120**, 2870–2879; C. Cañada-Vilalta, T. A. O'Brien, E. K. Brechin, M. Pink, E. R. Davidson and G. Christou, *Inorg. Chem.*, 2004, **43**, 5505–5521.
2 R. W. Saalfrank, I. Bernt, E. Uller and F. Hampel, *Angew. Chem., Int. Ed. Engl.*, 1997, **36**, 2482–2485; A. Caneschi, A. Cornia and S. J. Lippard, *Angew. Chem., Int. Ed. Engl.*, 1995, **34**, 467–469; K. L. Taft, C. D. Delfs, G. C. Papaefthymiou, S. Foner, D. Gatteschi and S. J. Lippard, *J. Am. Chem. Soc.*, 1994, **116**, 823–832; A. Caneschi, A. Cornia, A. C. Fabretti and D. Gatteschi, *Angew. Chem., Int. Ed.*, 1999, **38**, 1295–1297.
3 A. K. Powell, S. L. Heath, D. Gatteschi, L. Pardi, R. Sessoli, G. Spina, F. Del Giallo and F. Pieralli, *J. Am. Chem. Soc.*, 1995, **117**, 2491–2502.
4 C. Delfs, D. Gatteschi, L. Pardi, R. Sessoli, K. Wieghardt and D. Hanke, *Inorg. Chem.*, 1993, **32**, 3099–3103.
5 R. Shaw, R. H. Laye, L. F. Jones, D. M. Low, C. Talbot-Eeckelaers, Q. Wei, C. J. Milios, S. Teat, M. Helliwell, J. Raftery, M. Evangelisti, M. Affronte, D. Collison, E. K. Brechin and E. J. L. McInnes, *Inorg. Chem.*, 2007, **46**, 4968–4978.
6 A. Bino, M. Ardon, D. Lee, B. Spingler and S. J. Lippard, *J. Am. Chem. Soc.*, 2002, **124**, 4578–4579; O. Sadeghi, L. N. Zakharov and M. Nyman, *Science*, 2015, **347**, 1359–1362; G. W. Powell, H. N. Lancashire, E. K. Brechin, D. Collison, S. L. Heath, T. Mallah and W. Wernsdorfer, *Angew. Chem., Int. Ed.*, 2004, **43**, 5772–5775; C. Vecchini, D. H. Ryan, L. M. D. Cranswick, M. Evangelisti, W. Kockelmann, P. G. Radaelli, A. Candini, M. Affronte, I. A. Gass, E. K. Brechin and O. Moze, *Phys. Rev. B*, 2008, **77**, 224403; O. Nachtigall, M. Kusserow, R. Clérac, W. Wernsdorfer, M. Menzel, F. Renz, J. Mrozinski and J. Spandl, *Angew. Chem., Int. Ed.*, 2015, **54**, 10361–10364; A. E. Dearle, D. J. Cutler, H. W. L. Fraser, S. Sanz, E. Lee, S. Dey, I. F. Diaz-Ortega, G. S. Nichol, H. Nojiri, M. Evangelisti, G. Rajaraman, J. Schnack, L. Cronin and E. K. Brechin, *Angew. Chem., Int. Ed.*, 2019, **58**, 16903–16906; N. A. G. Bandeira, O. Sadeghi, T. J. Woods, Y.-Z. Zhang, J. Schnack, K. Dunbar, M. Nyman and X. Bo, *J. Phys. Chem. A*, 2017, **121**, 1310–1318.
7 G. Toulouse, *Comm. Phys.*, 1977, **2**, 115–119; S. Kirkpatrick, *Phys. Rev. B*, 1977, **16**, 4630–4641; A. P. Ramirez, *Annu. Rev. Mater. Sci.*, 1994, **24**, 453; O. Kahn, *Chem. Phys. Lett.*, 1997, **265**, 109–114; C. Schröder, H. Nojiri, J. Schnack, P. Hage, M. Luban and P. Kögerler, *Phys. Rev. Lett.*, 2005, **94**, 017205; J. Schnack, *Dalton Trans.*, 2010, **39**, 4677–4686; M. L. Baker, G. A. Timco, S. Piligkos, J. S. Mathieson, H. Mutka, F. Tuna, P. Kozłowski, M. Antkowiak, T. Guidi, T. Gupta, H. Rath, R. J. Woolfson, G. Kamieniarz, R. G. Pritchard, H. Weihe, L. Cronin, G. Rajaraman, D. Collison, E. J. L. McInnes and R. E. P. Winpenny, *Proc. Natl. Acad. Sci. U. S. A.*, 2012, **109**, 19113–19118; J. W. Sharples, D. Collison, E. J. L. McInnes, J. Schnack, E. Palacios and M. Evangelisti, *Nat. Commun.*, 2014, **5**, 5321; M. Murugesu, R. Clérac, W. Wernsdorfer, C. E. Anson and A. K. Powell, *Angew. Chem., Int. Ed.*, 2005, **44**, 6678–6682.
8 V. O. Garlea, S. E. Nagler, J. L. Zarestky, C. Stassis, D. Vaknin, P. Kögerler, D. F. McMorrow, C. Niedermayer, D. A. Tennant, B. Lake, Y. Qiu, M. Exler, J. Schnack and M. Luban, *Phys. Rev. B: Condens. Matter Mater. Phys.*, 2006, **73**, 024414.
9 M. I. Khan and J. Zubieta, *Prog. Inorg. Chem.*, 1995, **43**, 1–149.
10 R. H. Laye and E. J. L. McInnes, *Eur. J. Inorg. Chem.*, 2004, 2811–2818.
11 Y. Hou, X. Fang, K. D. Kwon, L. J. Criscenti, D. Davis, T. Lambert and M. Nyman, *Eur. J. Inorg. Chem.*, 2013, 1780–1787; E. Freire, M. Quintero, D. Vega and R. Baggio, *Inorg. Chim. Acta*, 2013, **394**, 229–236; A.-Q. Zhang and L.-L. Liu, *Transit. Met. Chem.*, 2017, **42**, 753–761.
12 W. Schmitt, L. Zhang, C. E. Anson and A. K. Powell, *Dalton Trans.*, 2010, **39**, 10279–10285.
13 A. Baniodeh, Y. Liang, C. E. Anson, N. Magnani, A. K. Powell, A.-N. Unterreiner, S. Seyfferle, M. Slota, M. Dressel, L. Bogani and K. Goß, *Adv. Funct. Mater.*, 2014, **24**, 6280–6290.
14 R. W. Saalfrank, I. Bernt, E. Uller and F. Hampel, *Angew. Chem., Int. Ed. Engl.*, 1997, **36**, 2482–2485.
15 L. F. Jones, P. Jensen, B. Moubaraki, K. J. Berry, J. F. Boas, J. R. Pilbrow and K. S. Murray, *J. Mater. Chem.*, 2006, **16**, 2690–2697.
16 O. Waldmann, R. Koch, S. Schromm, J. Schülein, P. Müller, I. Bernt, R. W. Saalfrank, F. Hampel and E. Balthes, *Inorg. Chem.*, 2001, **40**, 2986–2995; G. Xiong, Y.-L. Hou, J.-Z. Cui and B. Zhao, *Inorg. Chem. Commun.*, 2013, **35**, 89–91; A. M. Ako, O. Waldmann, V. Mereacre, F. Klower, I. J. Hewitt, C. E. Anson, H. U. Güdel and A. K. Powell, *Inorg. Chem.*, 2007, **46**, 756–766; O. Botezat, J. van Leusen, V. Ch. Kravtsov, A. Ellern, P. Kögerler and S. G. Baca, *Dalton Trans.*, 2015, **44**, 20753–20762; I. A. Gass, C. J. Milios, A. Collins, F. J. White, L. Budd, S. Parsons, M. Murrie, S. P. Perlepes and E. K. Brechin, *Dalton Trans.*, 2008, 2043–2053; M. Murugesu, K. A. Abboud and G. Christou, *Dalton Trans.*, 2003, 4552–4556.
17 T. Liu, Y.-J. Zhang, Z.-M. Wang and S. Gao, *J. Am. Chem. Soc.*, 2008, **130**, 10500–10501.
18 S.-J. Liu, S.-D. Han, J.-M. Jia, L. Xue, Y. Cui, S.-M. Zhang and Z. Chang, *CrystEngComm*, 2014, **16**, 5212–5215.
19 M. Murugesu, A. Mishra, W. Wernsdorfer, K. A. Abboud and G. Christou, *Polyhedron*, 2006, **25**, 613–625; O. Botezat, J. van Leusen, V. Ch. Kravtsov, P. Kögerler and S. G. Baca, *Inorg. Chem.*, 2017, **56**, 1814–1822.
20 J. Jaklič and P. Prelovšek, *Phys. Rev. B*, 1994, **49**, 5065–5068; J. Schnack and O. Wendland, *Eur. Phys. J. B*, 2010, **78**, 535–541; J. Schnack, J. Richter and R. Steinigeweg, *Phys. Rev. Res.*, 2020, **2**, 013186.
21 M. K. Singh and G. Rajaraman, *Inorg. Chem.*, 2019, **58**, 3175–3188; K. J. Mitchell, K. A. Abboud and G. Christou, *Inorg. Chem.*, 2016, **55**, 6597.
22 A. Baniodeh, N. Magnani, Y. Lan, G. Buth, C. E. Anson, J. Richter, M. Affronte, J. Schnack and A. K. Powell, *npj Quant. Mater.*, 2018, **3**, 10.
23 M. Coletta, S. Sanz, D. J. Cutler, S. J. Teat, K. J. Gagnon, M. K. Singh, E. K. Brechin and S. J. Dalgarno, *Dalton Trans.*, 2020, **49**, 14790–14797; M. Coletta, T. G. Tziotzi, M. Gray, G. S. Nichol, M. K. Singh, C. J. Milios and E. K. Brechin, *Chem. Commun.*, 2021, **57**, 4122–4125; S. Hazra, S. Bhattacharya, M. K. Singh, L. Carrella, E. Rentschler, T. Weyhermueller, G. Rajaraman and S. Mohanta, *Inorg. Chem.*, 2013, **52**, 12881–12892.

 This journal is © The Royal Society of Chemistry 2021